JACS
JOURNAL OF THE AMERICAN CHEMICAL SOCIETY
Article
pubs.acs.org/JACS

Dynamic Assembly and Disassembly of Functional β-Endorphin Amyloid Fibrils

Nadezhda Nespovitaya,[†,§] Julia Gath,[†] Konstantin Barylyuk,[‡,∥] Carolin Seuring,[†] Beat H. Meier,[†] and Roland Riek*[,†]

[†]Laboratory of Physical Chemistry, ETH Zurich, Vladimir-Prelog-Weg 2, 8093 Zurich, Switzerland
[‡]Laboratory of Organic Chemistry, ETH Zurich, Vladimir-Prelog-Weg 3, 8093 Zurich, Switzerland

Supporting Information

ABSTRACT: Neuropeptides and peptide hormones are stored in the amyloid state in dense-core vesicles of secretory cells. Secreted peptides experience dramatic environmental changes in the secretory pathway, from the endoplasmic reticulum via secretory vesicles to release into the interstitial space or blood. The molecular mechanisms of amyloid formation during packing of peptides into secretory vesicles and amyloid dissociation upon release remain unknown. In the present work, we applied thioflavin T binding, tyrosine intrinsic fluorescence, fluorescence anisotropy measurements, and solid-state NMR spectroscopy to study the influence of physiologically relevant environmental factors on the assembly and disassembly of β-endorphin amyloids in vitro. We found that β-endorphin aggregation and dissociation occur in vitro on relatively short time scales, comparable to times required for protein synthesis and the rise of peptide concentration in the blood, respectively. Both assembly and disassembly of amyloids strongly depend on the presence of salts of polyprotic acids (such as phosphate and sulfate), while salts of monoprotic acids are not effective in promoting aggregation. A steep increase of the peptide aggregation rate constant upon increase of solution pH from 5.0 to 6.0 toward the isoelectric point as well as more rapid dissociation of β-endorphin amyloid fibrils at lower pH indicate the contribution of ion-specific effects into dynamics of the amyloid. Several low-molecular-weight carbohydrates exhibit the same effect on β-endorphin aggregation as phosphate. Moreover, no structural difference was detected between the phosphate- and carbohydrate-induced fibrils by solid-state NMR. In contrast, β-endorphin amyloid fibrils obtained in the presence of heparin demonstrated distinctly different behavior, which we attributed to a dramatic change of the amyloid structure. Overall, the presented results support the hypothesis that packing of peptide hormones/neuropeptides in dense-core vesicles do not necessarily require a specialized cellular machinery.

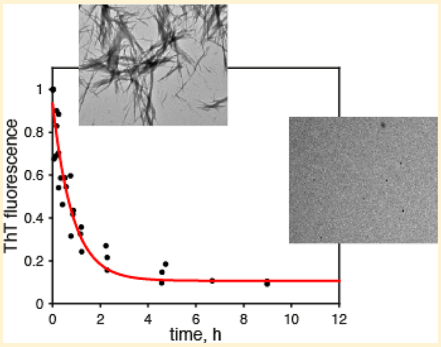

INTRODUCTION

Although the formation of amyloids is usually associated with protein misfolding diseases,[1] it can also be beneficial to organisms. Amyloids conferring an advantage to their host are classified as functional amyloids. Examples of efficient utilization of stable, rigid, and self-assembling amyloid structure are known from bacteria, yeast and fungi,[2−5] and mammals.[6,7]

Of interest here are mammalian functional amyloids formed by peptide hormones and neuropeptides,[8] which are vitally important messenger molecules responsible for the well-coordinated work of different cells and organs.[9,10] They are synthesized in the form of precursor polypeptides in secretory cells.[11] Precursors are enzymatically processed in the endoplasmic reticulum (ER) and Golgi complex (GC). Progressive processing and condensation of peptides lead to formation of dense-cored aggregates at the level of the trans-Golgi network.[12,13] These aggregates are eventually packed into dense-core vesicles (DCVs), which serve as a depot for temporary storage of peptide messengers in secretory cells. DCVs can be observed by electron microscopy (EM) as membrane-enclosed spherical organelles 180−200 nm in diameter with the electron-dense core material inside.[14−18] The amyloid nature of this material was hypothesized in early 1980s[19] and has been recently demonstrated experimentally.[8] Upon triggering, the material of DCVs is released into the blood or extracellular space,[12,13,18] which necessitates the amyloid disassembly for hormone/neuropeptide action. Therefore, the reversibility of peptide aggregation is a key property of functional hormone/neuropeptide amyloids and is essential for functional signal transduction in vivo.[20]

The exact molecular mechanism of peptide hormone/neuropeptide sorting in the secretory pathway remains highly debated.[12,13,21] Two alternative hypotheses propose "sorting by entry" and "sorting by retention". The first model suggests that secretory polypeptides aggregate with the assistance of a specialized protein machinery. For example, granins have been proposed as candidate components of such machinery that serve as sorting receptors and aggregation primers or seeds.[12,13,22] However, single deletions of the respective genes

Received: August 27, 2015
Published: December 23, 2015

DOI: 10.1021/jacs.5b08694
J. Am. Chem. Soc. 2016, 138, 846−856

do not stop the formation of DCVs, although the cargo processing and secretion can be significantly affected.[13] Moreover, specific receptors responsible for peptide hormone/neuropeptide sorting into the regulated secretory pathway have not been identified yet. The second model, "sorting by retention", proposes that polypeptides destined for regulated secretion are excluded from the active sorting due to the lack of any specific receptor. Upon further progression in the secretory pathway, they spontaneously aggregate and passively enter into DCVs.[13,21] Regardless of the sorting mechanism, it is evident that condensation of secretory polypeptides by aggregation alone is an effective method to exclude them from other sorting routes.[20]

Molecular mechanisms controlling the reversible formation of peptide hormone/neuropeptide amyloids are largely unknown. Notably, there are significant chemical, physical, and biological changes of the immediate environment in the secretory pathway along with the messenger peptide maturation and its packing into DCVs followed by the release from the secretory cell.[13,23−27] As reviewed in the following in more details, the major changes include (i) change in the local concentration of the hormone/neuropeptide, (ii) change in the buffer composition from polyvalent ions in the cytoplasm (such as phosphate) to monovalent ones in the blood, (iii) change in pH, and (iv) changes in the composition of carbohydrates, glycosaminoglycans, and proteins. Because hormones/neuropeptides have been evolutionarily optimized for secretory pathway, it is the working hypothesis that all of these changes may play an important role in the regulation of peptide aggregation and subsequent amyloid dissociation. Thus, the aim of this study is to evaluate the contribution in aggregation and dissociation of each of the following environmental changes.

The peptide content of DCVs experiences dramatic dilution when released from the cell. Neuropeptides are densely packed for storage in DCVs. For example, prolactin is 200× more concentrated in DCVs than in the ER.[14] Protein concentration in DCVs is estimated at 100−150 mg/mL,[21,28] whereas concentrations of neuropeptides in the blood range from 10 to 100 pg/mL.[29] Hence, the ultimate dilution factor can be as high as 10^9. However, neuropeptides act at the local level and diffuse just a few micrometers away from the secretory cell to evoke a response in neighboring cells.[18] The initial dilution occurs into the volume that is a factor of 10^6 greater than the volume of a single DCV, assuming its radius being equal to 100 nm and an average distance of 10 μm to a target. Provided that a secretory cell releases the content of several tens to hundreds of DCVs in response to a stimulus,[30] and several tens to hundreds of cells are activated at once, the actual dilution factor shall be even lower, but probably is still on the order of thousands of times.

Analysis of biological fluids demonstrates asymmetric distribution of mono- and polyvalent ions. For example, multiply charged anions are quite abundant inside the cell while monovalent anions and cations are plentiful in the blood and interstitial fluid. The level of phosphate is one of the highest in the cell and corresponds to 60 mM, whereas it drops down to 1−2 mM in the extracellular environment. Bicarbonate at a concentration of 24−28 mM is the major buffering system in the blood.[31,32] Therefore, one of the possible factors that may be involved in the dynamic assembly and disassembly of functional peptide amyloids is the change of electrolyte composition in the environment.

Another potentially important factor is the pH, which changes from 7.4 in the ER to 5.5 in secretory vesicles,[33] and back to 7.4 in the blood and interstitial space.[31] Notably, McGlinchey et al.[34] demonstrated the dissociation of amyloid fibrils formed by the repeat domain of Pmel17 upon pH change. However, the dissociation was rather slow and occurred on a time scale of more than 12 h.

Carbohydrates and glycosaminoglycans (GAGs) may also be involved in hormone/neuropeptide aggregation.[8,35] GAG heparin in combination with mannitol has been shown to promote amyloid aggregation in a large number of peptide hormones and neurotransmitters.[8] Various sugars are highly abundant in the ER and GC, which are the main locations of carbohydrate synthesis and protein glycosylation in mammalian cells.[11] GAGs being components of intracellular proteoglycans have been identified as relatively inert constituents of secretory vesicles in a wide range of cells where they mediate storage of other granule components. Upon secretion, GAGs can play a role in the protection, delivery, and presentation of the active components.[36] The composition of carbohydrates in different subcellular compartments including the ER, GC, and secretory vesicles is highly dynamic, and their exact abundances are poorly documented in the literature, so that only rough estimates can be given. For example, both blood and intracellular levels of glucose are maintained at 5 mM.[10,32] In the work of Lagunoff and co-workers,[37] secretory vesicles purified from 2 to 3 × 10^6 mast cells contained 9.8 μg of heparin, which corresponds to an intracellular concentration of 0.01−100 mM depending on the cell volume (100−10000 μm^3)[10,32] and the molecular weight of heparin (5000−40 000 Da)[38,39] chosen for the calculation. Interestingly, the purified granule material also contained 8 μg of protein.[37] However, the level of heparin in the blood plasma is estimated at 1−2.4 mg/L, i.e., from 25 nM to 1 μM.[40]

In order to evaluate these possible environmental contributors in the regulation of hormone/neuropeptide aggregation and disaggregation, we studied their influence on the aggregation and dissociation of β-endorphin amyloid in vitro. β-Endorphin is a 31-amino-acid-residue-long endogenous opioid neuropeptide involved in regulation of pain perception and stress response.[41,42] Increased levels of β-endorphin are found upon long-term physical and emotional stress,[43] in response to a high level of acetaldehyde following ethanol consumption,[44] as well as in patients with silent myocardial ischemia.[41] It also stimulates interleukine-4 secretion by T-lymphocytes.[45] A decreased level of β-endorphin is associated with migraine.[46] Reduction of the concentration of β-endorphin in the blood is essential for inducing maternal behavior.[41] β-Endorphin is synthesized in the adenohypophysis as a part of a larger precursor polypeptide pro-opiomelanocortin (POMC), which also gives rise to several other peptide hormones and neurotransmitters including adrenocorticotropic hormone (ACTH) and α-, β-, and γ-melanotropins.[47] The processing of POMC starts in the ER with cleavage of the N-terminal signal peptide and proceeds further in trans-Golgi network, where it is specifically cut into pro-ACTH and β-lipotropin. The latter is sorted into secretory vesicles and is eventually converted into β-endorphin, which is packed and stored in the form of functional amyloid inside mature DCVs.[12,47]

Herein, we studied reversible aggregation of β-endorphin in vitro at near-physiological conditions, and demonstrated the kinetics to be close to characteristic biological times. Important contributors in these processes are the concentration of β-

DOI: 10.1021/jacs.5b08694
J. Am. Chem. Soc. 2016, 138, 846−856

endorphin, the change from a polyvalent to a monovalent anion in the buffer solution, and the presence of heparin. These data shed light on the mechanisms of reversible hormone/neuropeptide aggregation and illustrate how changes of the immediate environment along the secretory pathway may guide these processes autonomously.

RESULTS AND DISCUSSION

Thioflavin T Binding Assay for Monitoring β-Endorphin Aggregation. The peptide aggregation was monitored over time by two complementary methods in parallel: ThT fluorescence and light absorbance at 600 nm, which was used as a measure of turbidity.[48] The experiments were performed in a 96-well plate format, which allowed for simultaneous measurements of several experimental conditions in the same plate. The enhancement of ThT fluorescence is an often used tool to monitor protein aggregation,[49−53] and the presence of the dye in the reaction mixture does not usually affect the aggregation.[54] However, in some cases, ThT can influence the aggregation kinetics by reducing the lag phase of the aggregation.[55] Therefore, to test the effect of ThT on the aggregation of β-endorphin, we performed control experiments, where the aggregation in the absence of ThT was monitored by turbidity only. Direct comparison of the turbidity profiles in the absence and presence of ThT revealed no significant differences (Figure S1). Another limitation of ThT as a reporter of amyloid fibril formation is that some amyloid fibrils do not bind and/or increase the fluorescence intensity of ThT,[56] whereas some amorphous aggregates lacking the fibrillar structure can increase ThT fluorescence and demonstrate other amyloid-specific features, such as Congo red binding and characteristic X-ray diffraction pattern.[57] However, in our study, all ThT-positive aggregates possessed fibrillar morphology, and all fibrils found under the EM were ThT-positive, as well as no amorphous aggregates were found in any sample (Figure S2).

Within the context of the experiments, it is also important to note that ThT has quite high affinity to amyloids (K_d in sub- to low-μM range), and the binding kinetics is faster than the time resolution of our assays (binding is complete within 30 s), which renders it a very sensitive reporter of amyloid structure.[58] ThT is a cationic dye and hence does not compete with inorganic/organic anions for binding to amyloids. In addition, we performed control steady-state measurements of ThT fluorescence intensity dependence on the concentration of stable amyloids in solution, which revealed a linear relationship (Figure S3). Furthermore, in the range of pH and ionic strength of solution used in our experiments, ThT is known to have stable photophysical properties.[58,59]

In addition, as discussed in the appropriate sections, the dissociation of β-endorphin amyloid was found to be unaffected by the presence of 15 μM ThT in the reaction mixture.

Multivalent Anions Promote Formation of β-Endorphin Amyloids. Salts are known promoters of protein aggregation.[60−63] Three major concepts explain ion effects on protein solubility and aggregation: the Hofmeister effect, the Debye−Hückel screening, and specific ion binding.[60−62]

In the initial screening of the influence of salts on the aggregation of β-endorphin, we found that multiply charged anions, such as phosphate, sulfate, and citrate, which are present in the cell in a relatively high abundance compared to extracellular fluids (up to 60 mM, 10 mM, and ∼1 mM, respectively),[31,32,64] can effectively promote β-endorphin aggregation, as evidenced by EM and ThT binding assay (Figures 1 and S2, and Table S1). Moreover, no additional factor was required to induce β-endorphin aggregation when

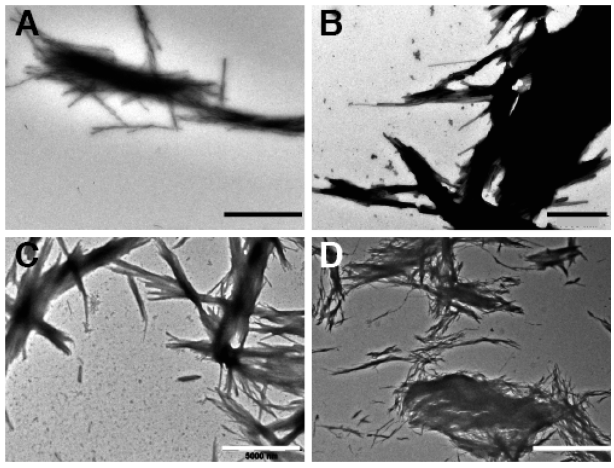

Figure 1. Electron micrographs of β-endorphin fibrils promoted by 10 mM sodium sulfate in 10 mM ammonium acetate, 200 mM sodium chloride, pH 5.5 (A), 50 mM sodium phosphate, pH 7.5 (B), 10 mM sodium citrate, pH 5.5 (C), and 50 mM Tris-maleate, pH 7.4 (D). Scale bars are 5 μm in A, C, D and 1 μm in B. EM images were obtained on 3-day-old samples of 2 mg/mL β-endorphin fibrillized at +37 °C.

salts of polyprotic acids were present. In contrast, buffers based on salts of monoprotic acids, such as ammonium acetate pH 5.5 or Tris-HCl pH 7.4, did not promote β-endorphin aggregation (Figure S2, Table S1).

Fibrils obtained in buffers containing different multivalent anions shared similar morphology in EM (Figures 1 and S2). They tended to form large bundles of laterally associated fibrils of several micrometers in length. The structures of salt-induced fibrils obtained in the presence of different multivalent anions were also probed at the atomic level by solid-state NMR spectroscopy, which did not reveal any significant structural difference. As exemplified by Figure S4, the two $^{13}C—^{13}C$ 2D DARR spectra[65] measured for β-endorphin fibrils formed either in a phosphate or citrate buffer are very similar. The superposition of the two spectra shows a nearly complete overlap of peaks, indicating a high structural similarity between the two samples.

Investigation of β-endorphin aggregation dependence on the amount of phosphate showed that 1 mM phosphate added to 10 mM Tris-HCl buffer at pH 7.4 was sufficient to promote amyloid formation, while no fibrils were detected at 100 μM phosphate concentration and lower (Table S1). Substitution of phosphate by 150 mM NaCl did not yield amyloid fibrils in a 24-h study. This difference in aggregation promotion effects cannot be attributed solely to the Debye−Hückel screening, because the ionic strength of solution was greater in the case of 10 mM Tris-HCl with 150 mM NaCl. Furthermore, as we demonstrate below, β-endorphin aggregation kinetics in the presence of phosphate exhibits a pronounced dependence on solution pH suggesting that specific ion effects contribute substantially to the mechanism of aggregation.[66] Specific ion binding is also unlikely since β-endorphin fibrils obtained in the presence of different salts (phosphate, citrate, or both mixed together) have very similar solid-state NMR spectra (Figures S4 and S5), hence, similar structures. Therefore, anions promote aggregation of β-endorphin in some indirect way, e.g., by

DOI: 10.1021/jacs.5b08694
J. Am. Chem. Soc. 2016, 138, 846−856

changing its interactions with water, which is more consistent with the Hofmeister effect. This notion is further supported by the finding that the amyloid-promoting effect of the tested salts correlates qualitatively with the Hofmeister series of anions (citrate > sulfate > phosphate > acetate > chloride):[67] after incubation for 24 h, fibrils were found only in those samples that contained citrate, sulfate, and phosphate, i.e., anions exerting a relatively strong Hofmeister effect (Table S1 and Figure S2).

β-Endorphin Aggregation Kinetics Depends on Solution pH and Correlates with the Peptide Charge State. The change in pH of intracellular compartments along the secretory pathway was proposed as one of the triggers responsible for hormone/neuropeptide aggregation and dissociation in vivo.[14,21] While there is acidification from the ER (pH 7.4) via GC (pH 6.0−6.7) to secretory vesicles (pH 5.5),[33] the blood pH is again maintained at 7.4.[31] To investigate the role of pH in the aggregation of β-endorphin, the buffer solution containing 50 mM sodium phosphate and 2 mM sodium citrate (termed CP buffer) was used for fibrillization of β-endorphin. This buffer system allows for working in a wide pH range[68] conveniently covering the normal biological pH values between 5.5 and 7.4. Moreover, phosphate at 50−70 mM concentration was identified among other low-molecular weight constituents of DCVs.[23,69]

The peptide aggregation was monitored over time by two complementary methods in parallel: ThT fluorescence and light absorbance at 600 nm, which was used as a measure of turbidity.[48] The tested pH values were systematically varied from 5.0 to 8.0 by increments of 0.5 pH unit. β-Endorphin aggregation was reproducibly detected by the increase of the ThT fluorescence intensity over time at pH 5.5 and higher within a few hours (Figure 2A). Curves representing the turbidity of aggregation mixtures followed the same trend as the ThT fluorescence intensity (Figure 2B). With increasing pH the aggregation rate increased and the lag phase of aggregation became shorter. At pH 6.0, β-endorphin amyloid formation occurred in less than 2 h. Interestingly, the measured aggregation times are comparable with the average duration of protein synthesis in eukaryotes (2−3 h). Thus, it can be speculated that the aggregation proceeds on a biologically relevant time scale.

The steepness of the exponential phase of β-endorphin aggregation curve rises dramatically upon increase of pH from 5.5 to 6.0, while the lag phase shortens significantly. In contrast, the aggregation of β-endorphin proceeds with approximately the same kinetics at pH 6.0 and above (Figure 2).

The similarity of aggregation curves measured at pH 6.0−8.0 and their difference from those measured at pH 5.5 can be explained by the charge state of β-endorphin in solution. According to a theoretical titration curve,[70] β-endorphin bears 3 positive charges in the interval between pH 6.0 and 8.0 (Figure S6). The curve has an inflection point at pH 5.5 where the charge of the peptide increases steeply from +3 to higher values at lower pH. The correlation between the theoretical titration curve and the tendency for aggregation suggests that the aggregation of β-endorphin in the given buffer condition is at least in part determined by its net charge.

LMW Carbohydrates Promote β-Endorphin Aggregation Similarly to Multivalent Anions. High concentrations of LMW carbohydrates and GAGs in the GC and secretory vesicles suggest that they may be involved in the process of peptide sorting and packing into DCVs.[36] Studies of protein

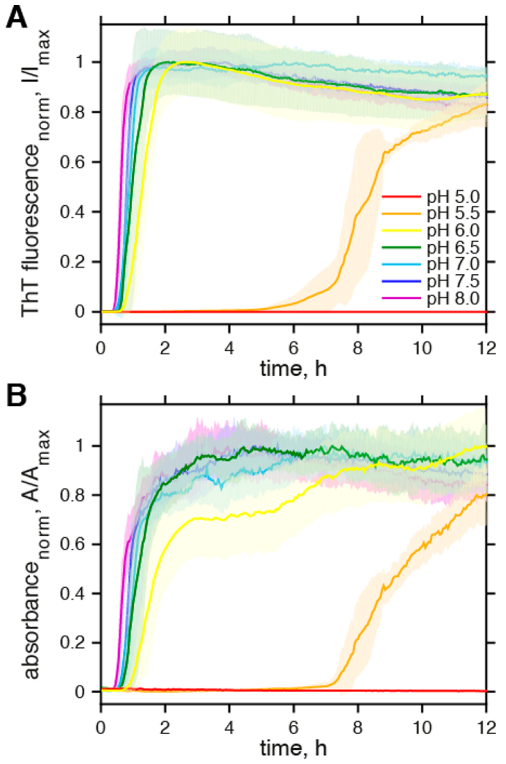

Figure 2. Time-resolved aggregation of β-endorphin with a monomer concentration of 2 mg/mL at +37 °C in the buffer solution containing 50 mM sodium phosphate and 2 mM sodium citrate adjusted to different pH: 5.0 (red, n = 9), 5.5 (orange, n = 9), 6.0 (yellow, n = 50), 6.5 (green, n = 10), 7.0 (cyan, n = 10), 7.5 (blue, n = 10), and 8.0 (purple, n = 10). Error bars show the standard deviations for each set of data. Number of replicas n is given in brackets. (A) The aggregation was monitored by the ThT fluorescence intensity. (B) The aggregation was monitored by the absorbance at 600 nm.

aggregation in the presence of carbohydrates in vitro showed that sugars affect aggregation of various proteins differently. For instance, glucose enhanced the nucleation of Aβ,[71] while glucagon aggregation in the presence of glucose was not significantly affected.[72] Many studies demonstrated that ionic carbohydrates of high polymerization degree, such as heparan sulfate and heparin, prompted dramatic changes in protein aggregation behavior upon addition.[8,51,52,73−75]

We tested the effect of several LMW carbohydrates (heparin-derived disaccharide I−S, glucosamine-6-sulfate, glucosamine, glucose), mannitol (Scheme S1), and heparin on β-endorphin aggregation in 10 mM ammonium acetate, 200 mM NaCl buffer, pH 5.5, and in CP buffer, pH 6.0. Heparin and protein were found in approximately equal amounts in DCVs.[37] We therefore added 2 mg/mL heparin to the aggregation mixture, which roughly corresponds to a molar concentration of 400 μM of 5-kDa heparin. Maji et al.[8] previously suggested that this concentration mimics the environment of secretory pathway. Similar concentration was also used in some other studies of heparin-induced protein aggregation.[51,75,76] Concentrations of LMW carbohydrates were also adjusted to 2 mg/mL, i.e., 8−10 mM (3 mM for heparin disaccharide I−S), in order to match the number of monosaccharide units in a generic 5-kDa heparin chain and account for cumulative ionic and osmotic properties of the polymer.[52]

The addition of all carbohydrates stimulated aggregation of β-endorphin in the ammonium acetate buffer, in which the

DOI: 10.1021/jacs.5b08694
J. Am. Chem. Soc. 2016, 138, 846−856

peptide did not normally aggregate on a time scale of 24 h (Figure S2 and Table S1). In turn, none of the tested additives, except heparin, led to any significant changes in the peptide aggregation behavior in CP buffer (Figure 3). β-Endorphin

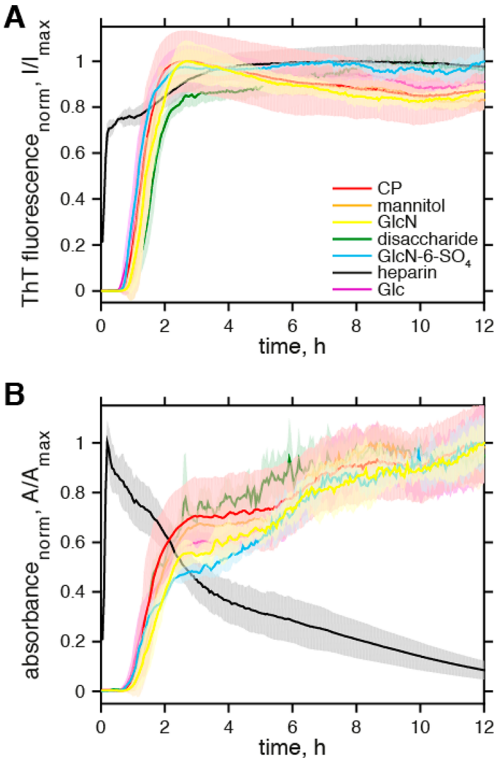

Figure 3. Time-resolved aggregation of β-endorphin with a monomer concentration of 2 mg/mL at +37 °C in 50 mM sodium phosphate and 2 mM sodium citrate buffer, pH 6.0, alone (red, n = 50) and in the presence of heparin (black, n = 9), heparin disaccharide I−S (green, n = 4), glucosamine-6-sulfate (cyan, n = 5), glucosamine (yellow, n = 10), glucose (purple, n = 10), and mannitol (orange, n = 10). All additives were used at the final concentration of 2 mg/mL. Error bars show the standard deviations for each set of data. Number of replicas n is given in brackets. (A) The aggregation kinetics was monitored by the ThT fluorescence intensity. (B) The aggregation kinetics was monitored by the absorbance at 600 nm.

aggregation in the presence of heparin was different from the course of salt-induced aggregation in CP buffer. (i) There was no lag phase, and (ii) the initial rapid increase in ThT fluorescence intensity was followed by a short break for 30 min, after that the signal continued to grow slowly within the next 4−5 h until reaching a plateau. Very similar biphasic aggregation kinetics were reported previously for peptide hormone kisspeptin-10 aggregated in the presence of heparin.[51] (iii) In the turbidity measurements, maximal absorbance rapidly developed in the heparin-containing samples within the first 30 min of aggregation and was followed by a decrease down to 10% of the maximum (Figure 3). (iv) At the end of the aggregation assay, the wells with heparin contained transparent jelly-like material, unlike samples with LMW carbohydrates. (v) Subsequent examination of heparin-induced β-endorphin fibrils by EM showed that they have a distinct morphology. Unlike the salt-promoted fibrils (Figure 1), the heparin-induced ones were well separated from each other and had a much greater length, up to several micrometers (Figure S2).

The difference in the course of aggregation and morphology observed for heparin-promoted β-endorphin fibrils hinted toward a potentially different atomic structure. We measured a $^{13}C—^{13}C$ 2D DARR spectrum of these fibrils and compared it to the spectrum of salt-promoted aggregates. Indeed, superposition of the spectra revealed significant differences in the number and positions of peaks (Figure S7). For instance, the Glu8 Cδ atom had an unusually low chemical shift of 175.3 ppm in the case of heparin-induced fibrils.[77] This chemical shift was attributed to a protonated form of the glutamic acid residue side chain.[78] In the case of salt-induced β-endorphin fibrils, the sample was polymorphic: at least four resonances were found for the Cδ of Glu8 spreading between 181 to 183 ppm (Figure S7B), which corresponds to a deprotonated state of the Glu8 side chain.[78]

However, the comparison of the DARR spectra of β-endorphin fibrils obtained in CP buffer alone and in the presence of heparin disaccharide I−S or glucosamine-6-sulfate, which are the building blocks of heparin, showed that they overlap very well (Figures S8 and S9). In other words, LMW constituents of heparin did not influence the aggregation kinetics of β-endorphin and the structure of fibrils in the same way as heparin. Moreover, the DARR spectrum of β-endorphin fibrils obtained in the presence of heparin disaccharide I−S in the ammonium acetate buffer, which does not promote aggregation alone, was also very similar to that of salt-promoted fibrils (Figure S10).

The high structural conservatism of functional β-endorphin amyloid fibrils regardless of the type of aggregation promoter (with the exception of heparin), be it salts of polyprotic acids or LMW carbohydrates, suggests that β-endorphin aggregation is not prone to environment-dictated polymorphism. Only upon addition of heparin a different structure is obtained indicating that heparin may engage into some direct interaction with the peptide leading to the amyloid with a distinct structure. Curiously, the promotion of amyloid formation by heparin was previously attributed to molecular crowding effect,[79,80] but our data suggest alternative explanation for the case of β-endorphin.

Fast Disassembly of β-Endorphin Amyloids. To probe the buffer conditions influencing fibril disassembly, we developed a method to monitor the dissociation of β-endorphin fibrils in solution. The method comprises the ThT binding assay to detect amyloid in the bulk phase and the measurement of Tyr intrinsic fluorescence in the soluble fraction of the reaction mixture to detect products of the dissociation reaction (Scheme S2). The dissociation solution contained 10 mM Tris-HCl buffer adjusted to pH 7.4, mimicking the pH and prevalence of salts of monoprotic acids in the blood. Notably, a prolonged incubation of β-endorphin in this buffer did not yield amyloid fibrils[8] (Table S1). Fibrils were collected by centrifugation, transferred to the 50-fold greater volume of the dissociation buffer, and incubated under stirring at room temperature. Aliquots were taken from the dissociation mixtures at different time points and mixed with ThT for fluorescence measurements. Another set of aliquots was subjected to ultracentrifugation, and the obtained supernatants were directly used for measurements of the Tyr fluorescence. Remarkably, the age of β-endorphin amyloid fibrils was found to be a critical parameter. Prolonged incubation of the peptide under the aggregation conditions yielded fibrils that exhibited much less reproducible dissociation kinetics. The age of fibrils used in all of the dissociation experiments reported below was therefore standardized to 2−4 days in order to minimize

DOI: 10.1021/jacs.5b08694
J. Am. Chem. Soc. 2016, 138, 846−856

variability of the measured dissociation kinetics. It is noteworthy that DCVs aging reduces the probability of their content secretion in response to a stimulus in vivo. For instance, in bovine adrenal chromaffin cells, the lifespan of atrial natriuretic factor-containing DCVs is 18 days, but only the youngest (<48 h) DCVs are secreted upon stimulation.[30]

The EM examination of the samples of salt-induced β-endorphin fibrils before and after a 24-h dissociation assay revealed almost complete disappearance of fibrillar material (Figure 4A,B). The ThT fluorescence intensity measurements

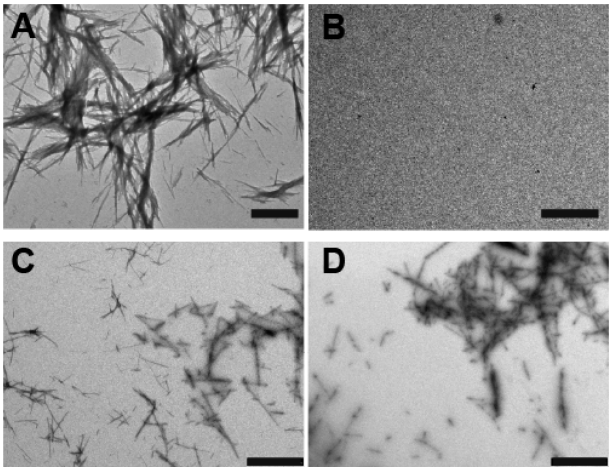

Figure 4. Electron micrographs of β-endorphin fibrils obtained from 50 mM sodium phosphate and 2 mM sodium citrate buffer, pH 6.0, alone (A) and in the presence of 2 mg/mL of heparin (C). The peptide at a concentration of 2 mg/mL was incubated at +37 °C for 2 days. Prior to EM imaging, β-endorphin fibrils were diluted 50-fold by the fibrillization buffer (A, C). Electron micrographs of the salt-induced (B) and heparin-promoted (D) β-endorphin fibril samples subjected to the dissociation assay (i.e., centrifugation and subsequent buffer exchange into 10 mM Tris-HCl, pH 7.4, by resuspension of the aggregates at 50-fold dilution) for 24 h. Scale bars are 2 μm.

demonstrated pronounced decay over time indicating the decrease of amyloid content in the reaction mixture (Figure 5A). Fibril disassembly occurred on a relatively short time scale with a decay constant of 0.86 ± 0.23 h (the decay constant is defined as the time when the ThT fluorescence intensity was reduced e-fold relative to its initial value) (Table S2 and Figure S11A). The simultaneous monitoring of the Tyr fluorescence revealed a rapid buildup of the signal intensity with a similar time constant of 1.16 ± 0.41 h (the time when Tyr fluorescence intensity increased e-fold relative to its initial value) reflecting the release of soluble β-endorphin from the amyloid fibrils (Figures 5B and S11B). The origin of the Tyr fluorescence signals from β-endorphin was confirmed by analytical RP-HPLC followed by mass spectrometric analysis (Figure S12). The dissociation assay was independently repeated multiple times for samples from the same and different batches of salt-induced β-endorphin fibrils and consistently gave reproducible results.

The exponential decay of the amyloid content together with the exponential rise of soluble β-endorphin in the dissociation assay suggest pseudo-first-order kinetics of β-endorphin fibril disassembly limited by the dissociation rate of the monomers from the fibril ends. Disassembly of each fibril may thus be attributed to a sequential detachment of monomers from fibril termini with a constant rate (Scheme S3). That being said, such

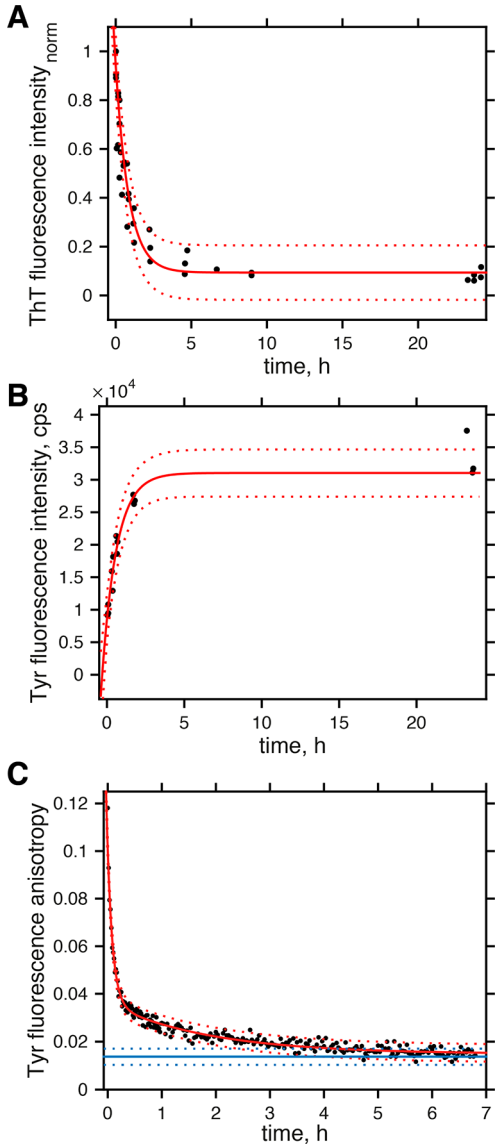

Figure 5. Time-resolved fibril dissociation assay carried out for β-endorphin fibrils in 10 mM Tris-HCl buffer, pH 7.4, diluted 50 times from the fibrillization buffer. The buffer exchange was done by centrifugation and resuspension of the amyloid pellet. The fibrils were obtained from 50 mM sodium phosphate and 2 mM sodium citrate buffer, pH 6.0, at +37 °C and a monomer concentration of 2 mg/mL. Black dots represent experimental data. The results of three independent replicas are shown. The lines of the best fits are shown in red (solid lines) with 95% confidence intervals (dotted lines). (A) ThT fluorescence intensity over time monitored off-line. The decay of the ThT fluorescence indicates the reduction of amyloid content. (B) Intrinsic Tyr fluorescence in the supernatant monitored over time off-line. The rapid increase of the Tyr fluorescence indicates the appearance of soluble β-endorphin. (C) Tyr fluorescence anisotropy measurement performed online. The fibril sample was diluted 100 times. The change of the fluorescence anisotropy reflects dissociation of β-endorphin fibrils. The Tyr fluorescence anisotropy of monomeric β-endorphin at a concentration of 0.02 mg/mL in 10 mM Tris-HCl buffer (pH 7.4) is shown as solid blue line. Blue dotted lines represent the standard deviation of measurements (n = 9).

a two-state reaction scheme is certainly an oversimplified model of the amyloid dissociation mechanism. It does not account for any higher-order structure of fibrils that may affect the release

DOI: 10.1021/jacs.5b08694
J. Am. Chem. Soc. 2016, 138, 846−856

of monomers, or potential occurrence of oligomeric intermediates.

The fibril disassembly was further monitored by fluorescence anisotropy as a measure of molecular mobility.[81,82] Since the extent of the Tyr fluorescence anisotropy is dependent on the structural state of the Tyr side chain it was hypothesized that the conformational change from the amyloid state to the soluble state of β-endorphin should be detectable by fluorescence anisotropy. The strength of this method is that it allows for a dye-free monitoring of fibril disassembly. In this experiment, the pellet consisting of salt-induced β-endorphin fibrils was resuspended in the dissociation buffer and left under constant stirring in the measurement cell of a fluorometer allowing for continuous online monitoring of the Tyr fluorescence anisotropy (Scheme S4). As demonstrated in Figure 5C, the measured fluorescence anisotropy decreased exponentially over time. The level of Tyr fluorescence anisotropy at the end of the dissociation assay was comparable with the signal from monomeric β-endorphin (Figure 5C, blue line), reflecting the fact that the fraction of monomeric peptide was approaching 100%. The determined decay constant overall agreed with the time constants obtained in the ThT binding and Tyr intrinsic fluorescence assays. Actually, the signal decay observed in this experiment was faster than the ThT fluorescence intensity decay and Tyr intrinsic fluorescence increase monitored off-line. We attributed this finding to unequal sample mixing in the off-line and online experiment formats. In addition, the measurement of Tyr fluorescence anisotropy could capture two exponential components of the dissociation reaction kinetics (Figure S11C−E) with time constants of 0.098 ± 0.008 h and 1.88 ± 0.29 h (Table S2). The emergence of the second exponential term points to a more complex dissociation mechanism, which may involve accumulation of oligomeric intermediates in the reaction mixture and/or contribution of the reverse process of fibril assembly.

Our results show without any ambiguity that salt-induced β-endorphin amyloid fibrils do disassemble upon transfer to the dissociation buffer. Replacement of multivalent phosphate and citrate anions with monovalent chloride anions in combination with dilution of the fibrillar material in the dissociation buffer is sufficient to trigger fast spontaneous disassembly of β-endorphin amyloids. The good agreement of the results of the ThT binding, Tyr intrinsic fluorescence, and Tyr fluorescence anisotropy assays suggests that any of the three methods can be used to specifically monitor fibril dissociation. Hence, we opted to utilize for the following experiments the ThT binding assay with online detection directly in the optical measurement cell of the fluorometer as the most convenient approach to further study β-endorphin amyloid disassembly under various conditions.

Influence of Additives on the Disassembly of β-Endorphin Amyloids. Probing the disassembly of β-endorphin fibrils obtained in the presence of LMW carbohydrates by ThT binding assay (with the online readout approach) revealed that they feature dynamic properties very similar to salt-induced aggregates (Figures S13−S15 and Table S2). This finding is very well in line with the fact that all these aggregates share a similar structure, as evidenced by NMR spectroscopy (see above). The only type of β-endorphin amyloid aggregates that behaved differently in the dissociation assay and also formed a different structure when compared to the salt-induced aggregates (see above) was the heparin-induced fibrils. They had slower dissociation kinetics on the time scale of experiment (Figure S13, black trace). In the off-line assay monitored over 24 h, the ThT fluorescence intensity decreased by approximately 10−15% (Figure S16A), consistently with the increase of Tyr intrinsic fluorescence intensity in the soluble fraction (Figure S16B). The Tyr fluorescence anisotropy value in the online monitored assay scatters around 0.11 with the standard deviation of 0.02 (Figure S16C). These data are in agreement with previously reported dissociation times of β-endorphin amyloid fibrils obtained in solution containing 2 mg/mL heparin and 5% mannitol. Maji et al.[8] observed the appearance of monomeric β-endorphin in the outer buffer after 100 h of dialysis of the fibrils in a dialysis unit with 10 kDa MWCO against 10 mM Tris-HCl, pH 7.4. Simultaneously, the ThT fluorescence measured in the sample solution decreased *e*-fold within 100 h of the experiment. Therefore, on the 24-h time scale of our experiment heparin-promoted fibrils of β-endorphin persisted the dissociation assay (Figure 4C−D).

All types of β-endorphin amyloid fibrils studied, with the exception of those obtained in the presence of heparin, demonstrated similar dissociation kinetics. Addition of LMW carbohydrates to the aggregation buffer did not affect the dissociation of β-endorphin amyloid upon transfer to 10 mM Tris-HCl buffer, pH 7.4. Hence, β-endorphin forms a truly dynamic functional amyloid capable of dissociation on a relatively short time scale irrespective of the type of salt or LMW carbohydrate that originally promoted fibril formation. Remarkably, the observed dissociation constant of approximately 20−50 min correlates with the time of 20−60 min needed to build up the maximal level of the peptide in the blood upon stimulation by physical exercise.[29,83]

Disassembly of β-Endorphin Amyloid Fibrils Is Affected by Phosphate Concentration, Dilution Factor, and pH. We performed experiments probing the effects of phosphate concentration, pH, and fibril dilution on amyloid disassembly similar to the investigation that examined the immediate environment's influence on β-endorphin fibril formation above. These parameters have been selected because, upon secretion of neuropeptides from DCVs into the blood/extracellular space, they exhibit dramatic changes. In the following, we systematically studied the influence of these parameters on the disassembly rate of β-endorphin fibrils using the dissociation assay with the online readout of the ThT fluorescence intensity (Figure 6).

As the concentration of sodium phosphate in the dissociation buffer was increased from 0 to 50 mM, the disassembly rate of β-endorphin fibrils consistently slowed down (Figure 6A). In details, the dissociation constant increased from 0.29 ± 0.01 h to 2.12 ± 0.08 h proportionally with the increase of phosphate concentration (Table S2 and Figures S17−S18). The fibril dissociation remained thereby reasonably fast at 10 mM phosphate, which is the expected equivalent concentration of multivalent anions (including phosphate) in the blood plasma.[31] It is further worth noting that the fibril disassembly at 50 mM phosphate is mostly due to the 50-fold dilution used in the assay (see below).

In order to investigate the pH-dependence of fibril disassembly, two time-resolved dissociation assays of β-endorphin fibrils at pH 5.5 and pH 7.4 with a 1:100 dilution in 50 mM ammonium acetate buffer were measured (Figure 6B). Consistent with the results of the pH-dependent aggregation experiments, the fibril disassembly was significantly

DOI: 10.1021/jacs.5b08694
J. Am. Chem. Soc. 2016, 138, 846−856

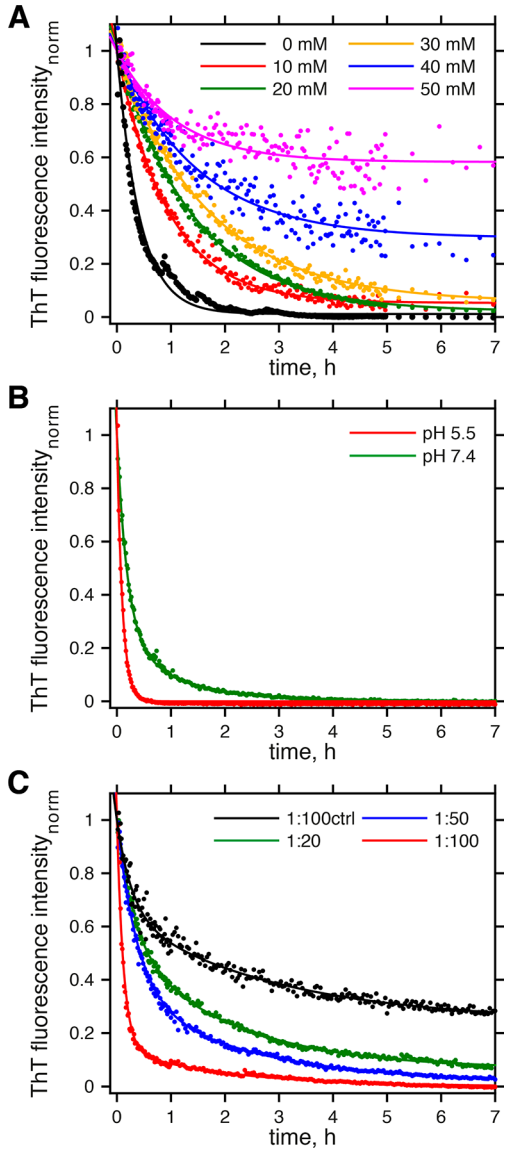

Figure 6. Influence of different buffer parameters (A: phosphate concentration, B: pH, and C: dilution) on the rate of β-endorphin fibrils dissociation monitored at +37 °C by the ThT binding assay with the online readout. (A) Time-resolved dissociation of β-endorphin fibrils in the presence of different concentrations of phosphate at 1:50 fibril dilution. Experimental data (dots) were fitted by a single exponential equation (curves). The various phosphate concentrations tested are indicated in the inset. (B) Time-resolved dissociation of β-endorphin fibrils at pH 5.5 (red) and pH 7.4 (blue) at 1:100 dilution in 50 mM ammonium acetate buffer. (C) Time-resolved dissociation of β-endorphin upon 20-, 50-, and 100-fold dilution in 10 mM Tris-HCl, pH 7.4 (green, blue, and red, respectively). The black curve (1:100ctrl) represents the evolution of the ThT fluorescence signal upon 100-fold dilution of β-endorphin fibrils in the fibrillization buffer (50 mM sodium phosphate and 2 mM sodium citrate, pH 6.0). In B and C, experimental data (dots) were fitted by a biexponential equation (curves). The fibrils were obtained from 50 mM sodium phosphate and 2 mM sodium citrate, pH 6.0, at +37 °C and at a monomer concentration of 2 mg/mL.

faster at pH 5.5 when compared to pH 7.4 (Figure 6B, Figures S19 and S20). The disassembly process at pH 5.5 was remarkably fast with a time constant of 0.101 ± 0.003 h. At pH 7.4 in turn, the extracted dissociation constants were 0.190 ± 0.004 and 1.06 ± 0.03 h (Table S2).

Finally, the implication of dilution on fibril disassembly was investigated. The importance of the dilution factor (which in the body may be several orders of magnitude) can already be seen in the control experiment (Figure 6C).

Dilution of β-endorphin fibrils obtained from CP buffer, pH 6.0, by the same fibrillization buffer at the ratio of 1:100 resulted in a relatively fast decrease of the ThT fluorescence intensity (0.28 ± 0.04 and 2.86 ± 0.27 26 h, dissociation constants) followed by a plateau at the level of approximately 30% of the initial signal intensity. The establishment of a new dynamic equilibrium between the amyloid state and free β-endorphin in solution supports further the reversible nature of β-endorphin amyloid aggregate. Even faster dissociation kinetics was registered when the fibrils were diluted in Tris-HCl buffer containing no phosphate (Figure 6C, Figures S21 and S22). Biexponential fitting of the experimental data (Figure S22) provided the following fast and slow dissociation constants: 0.074 ± 0.002 h and 1.4 ± 0.1 h, 0.29 ± 0.01 and 2.46 ± 0.13 h, and 0.31 ± 0.02 h and 2.0 ± 0.12 h for 1:100, 1:50, and 1:20 dilution, respectively (Table S2). The signal reached a plateau at a much lower level above the baseline reflecting more complete conversion of fibrils into soluble peptide in the absence of phosphate.

As we discussed above (see Figure 5C and associated discussion), the presence of two exponents points to a more complex mechanism of β-endorphin fibril disassembly than sequential irreversible monomer detachment from the termini of a fibril. Generally, multiple exponents reflect simultaneous presence of several fibril populations with different kinetic properties. Such heterogeneity can result from the following reasons: (i) fibril polymorphism, which has been observed in solid-state NMR spectra of salt-induced β-endorphin amyloid; (ii) the presence of higher-order structures, e.g., fibril bundles, which alter the ability of individual fibrils within the bundle to dissociate; (iii) fibrils constituted by various number of protofilaments; and (iv) accumulation of intermediates that bind ThT. We anticipate that both polymorphism as well as the abundance of higher order fibril associates, which increases with the age of sample, are most likely responsible for the observed double-exponential kinetics.

CONCLUSIONS

In the present work, we systematically studied the dynamic properties of functional β-endorphin amyloids. We employed several complementary methods including time-resolved ThT binding and Tyr intrinsic fluorescence assays, as well as steady-state EM and solid-state NMR spectroscopy to investigate fibril morphology and structure. Our data demonstrated that β-endorphin spontaneously aggregates in the presence of physiologically relevant concentrations of multivalent anions, such as phosphate or sulfate, and/or LMW carbohydrates. The amyloids formed exist in a dynamic equilibrium with the peptide monomer. The physiologically relevant change of the immediate environment (such as the peptide concentration, electrolyte composition, pH, and presence of additives) can shift this equilibrium between the fibrillar and soluble state. In our experiments, the aggregation took place in 2 h, while the dissociation rate constant ranged from as low as several minutes to 50 min, depending on the conditions of the experiments. The measured aggregation and dissociation rates are in agreement with time scales typical for protein synthesis in vivo as well as the time of 20−60 min required to reach maximal levels of the peptide in the blood upon stimulation by

DOI: 10.1021/jacs.5b08694
J. Am. Chem. Soc. 2016, 138, 846−856

physical exercise.[29,83] Functional β-endorphin amyloids promoted by various salts and LMW carbohydrates shared significant structural similarities as revealed by NMR spectroscopy. The only exception observed was the heparin-promoted fibrils, which exhibited a different aggregation behavior, a greater stability in the dissociation experiments, and featured a distinct structure.

Our results give an insight into the mechanism of functional hormone/neuropeptide aggregation. The measured rates of the amyloid fibril formation and dissociation were strongly affected by the global physicochemical properties of the system (the charge and concentration of the peptide, the presence and concentration of multivalent anions and sugars), and all the dependences found were monotonic. Following these findings, we suggest that ion-specific and osmotic effects are both driving forces of the peptide amyloid assembly and disassembly.

It is yet to be established how general the processes and effects described here for β-endorphin are for the other neuropeptides and hormones. Nevertheless, our findings suggest that the change of the immediate environment along the secretory pathway is sufficient to trigger amyloid aggregation. Therefore, spontaneous and reversible amyloid formation by the neuropeptide in response to changes in the surrounding medium supports the hypothesis that self-packing of proteins in DCVs occurs without the necessity of any cellular machinery.[21,25]

EXPERIMENTAL SECTION

Aggregation Kinetics in 96-Well Plates. ThT from Sigma (St. Louis, Missouri, U.S.A.) was dissolved in double-deionized water and filtered through a 0.2 μm pore size Filtropur S filter (SARSTEDT AG & Co., Germany). The dye concentration was determined by UV absorbance (ε_{412nm} = 36 000 $M^{-1}cm^{-1}$). A stock solution at 1.5 mM dye concentration was prepared and stored at −25 °C until use. Stocks of 200 mM dibasic sodium phosphate, 200 mM monobasic sodium phosphate, 1 M sodium citrate tribasic (Sigma-Aldrich Chemie GmbH, Buchs, Switzerland), and 1 M citric acid (Merck KGaA, Darmstadt, Germany) were prepared fresh before each experimental series. To prepare CP buffer solution, dibasic and monobasic sodium phosphate, citric acid and sodium citrate solutions were mixed in certain proportions (Table S3) to yield 50 mM concentration of phosphate, 2 mM concentration of citrate, and the desired pH.

Deionized water was distributed by aliquots of 200 μL into the wells surrounding those with the samples. Two mL of CP buffer were mixed with 20 μL of the 1.5 mM ThT stock solution. An 180-μL portion of this mixture was loaded into each well in the nonbinding, clear-bottom, black 96-well plate (cat. no. 655906, from Greiner Bio-One, Stonehouse, U.K.). Two mg peptide aliquots were dissolved in 1 mL of CP buffer. Ten μL of the 1.5 mM ThT stock solution was added to the peptide solution, mixed, and distributed by 180 μL in the 96-well plate. Each condition was present on a plate in 5 replicas. The measurement was repeated at least twice for each condition independently in two different plates using fresh material. The 96-well plate was sealed by AMPLiseal Transparent Microplate Sealer (made in the U.S.A., PN 676040 from Greiner Bio-One, Frickenhausen, Germany). Fluorescence measurements were performed on an Enspire 2300 Multilabel Plate Reader (PerkinElmer, Schwerzenbach, Switzerland). The temperature was set to +37 and +41 °C for the lower and upper heaters, respectively, to prevent condensation. The intensity of ThT emission at 485 nm was measured every 3 min in the bottom excitation/emission channel at a fixed focal height of 3 mm. The excitation was at 450 nm, with 50 flashes. The absorbance at 600 nm was measured with 20 flashes. Fluorescence and absorbance signals were collected from 5 different spots in the XY-plane and averaged. One fluorescence measurement, one absorbance measurement, and shaking for 55 s at 500 rpm in orbital mode after each measurement comprised one cycle. The cycle was repeated 480 times. Twenty-five wells were measured in each experiment.

LMW carbohydrates, including heparin disaccharide I−S sodium salt, D-glucosamine 6-sulfate (≥99%), D-(+)-glucosamine hydrochloride (≥99%), D-mannitol, all from Sigma-Aldrich (Buchs, Switzerland), and D-glucuronic acid (98%), D(+)-glucose, ACS reagent, anhydrous from Acros Organics (Fisher Scientific AG, Wohlen, Switzerland), were each dissolved in CP buffer (pH 6.0) at 100 mg/mL concentration. In order to account for the fact that heparin being a polymer exerts cumulative properties (polyelectrolyte, strong osmolyte), we added equivalent amounts of LMW saccharides based on the number of monosaccharide units in a generic 5-kDa heparin chain (sc-203075, Santa Cruz Biotechnology;[84]). Thus, the number of equivalents of, e.g., sulfate added with glucosamine sulfate matched that in heparin.[52] Furthermore, 8−10 mM concentrations of LMW saccharides (3 mM for heparin disaccharide I−S) fall into the same rage as the molarity of inorganic salts used in the present study. The test and blank samples were prepared as described above except the fact that the pH was always kept at 6.0. For the individual experiments, 3.6 μL of one LMW carbohydrate stock solution were added to the test and blank wells immediately before sealing the plate. Measurements were performed with the Enspire 2300 Multilabel Plate Reader as described above.

Dissociation Kinetics Measured Off-Line. 80 μL of β-endorphin amyloid fibrils obtained after incubation of the peptide in CP buffer for 2 days, pH 6.0, were centrifuged for 30 min at 2 × 10^4*g* and a temperature of +22 °C (Microcentrifuge 5417R, Vaudaux-Eppendorf AG, Schönenbuch/Basel, Switzerland). The pellets obtained were resuspended in 80 μL of 10 mM Tris-HCl (BiosolveBV Valkenswaard, Netherlands) buffer (pH 7.4) and subsequently diluted to 4 mL with the same buffer in 5 mL glass bottles closed by polypropylene caps. The dissociation mixture was kept at room temperature under constant stirring at 750 rpm on a magnetic stirrer plate. At different time points, samples were taken either for the ThT binding or for Tyr fluorescence measurements. For the ThT binding assay, 150 μL of the dissociation mixture were directly mixed with 1.5 μL of 1.5 mM ThT solution. ThT fluorescence spectra were recorded on a FluoroMax-4 spectrofluorometer controlled by FluorEssence software (Horiba Jobin Yvon GmbH, Munich, Germany). The excitation wavelength was set to 440 nm, and three spectra were acquired in the range of 460−550 nm utilizing 3 nm slits for excitation and emission. To monitor the appearance of free β-endorphin, 150 μL of the dissociation mixture were centrifuged for 30 min at 28 psi in the Airfuge Air-Driven centrifuge (Beckman Coulter International S.A., Nyon, Switzerland). The supernatant was collected and used to measure the intrinsic Tyr fluorescence. Tyr fluorescence spectra were recorded on the FluoroMax-4 spectrofluorometer. Excitation wavelength was fixed at 275 nm, and three spectra were acquired in the range of 290−500 nm utilizing 3 nm slits for excitation and emission. This experiment was repeated three times independently for three samples of β-endorphin fibrils obtained from the same batch. The β-endorphin identity was confirmed by analytical RP-HPLC of the soluble fraction obtained from the fibril dissociation assay. The retention time of β-endorphin was determined by injecting the peptide standard. The fraction corresponding to the major peak in the elution profile was analyzed by ESI-MS on a hybrid quadrupole/time-of-flight mass spectrometer (Synapt G2-S HDMS, Waters, Manchester, U.K.).

Dissociation Monitored Online by ThT Binding Assays. A 40-μL portion of the suspension of β-endorphin amyloid fibrils obtained after 2−4 days of incubation of the peptide in CP buffer at pH 6.0 was centrifuged at 2.0 × 10^4*g* and a temperature of +22 °C for 30 min. The pellet was resuspended in 10 mM Tris-HCl buffer adjusted to pH 7.4 in the volume of the starting material and transferred to 2 mL Tris-HCl buffer (pH 7.4) containing 15 μM of ThT in the fluorescent cuvette 111-QS (Hellma Analytics, Hellma Schweiz AG, Zumikon, Switzerland) with a stirrer bar and closed with a tight Teflon lid. 60 single-point measurements of ThT fluorescence were recorded every 1 min for the first hour, every 2 min for the next 4 h, and every 15 min for 19 h on the FluoroMax-4 spectrofluorometer. The excitation wavelength was fixed at 440 nm and the emission at 482 nm,

DOI: 10.1021/jacs.5b08694
J. Am. Chem. Soc. 2016, 138, 846−856

respectively, slits were set to 3 nm. From 3 to 10 single measurements were performed and averaged at each time point aiming at a standard deviation less than 2%. The dissociation mixture was under constant stirring at the maximum rate provided by FluoroMax-4. The measurement cell was kept at +37 °C controlled by the temperature bath (Compatible control CC3, Huber, Faust, Schaffhausen, Switzerland). Between measurements, the cuvette was extensively washed by deionized water and isopropanol. The cuvette was stored in 5% (v/v) solution of deconex 11 UNIVERSAL from Borer Lab (Dr. Grogg Chemie AG, Srettlen-Deisswil, Switzerland) at room temperature.

Dissociation Kinetics Monitored by Fluorescence Anisotropy. 40 μL of amyloid fibrils formed by incubation of β-endorphin in CP buffer at pH 6.0 for 2 days were centrifuged at 2.0×10^4 g and a temperature of +22 °C for 30 min. The pellet was resuspended in 40 μL of 10 mM Tris-HCl buffer at pH 7.4 and transferred to 2 mL Tris-HCl buffer (pH 7.4) in the fluorescent cuvette 111-QS, and closed with the tight Teflon lid. Fluorescence anisotropy was measured every 60 s for 1 h and every 120 s for the following 6 h by the FluoroMax-4 spectrofluorometer. The excitation and emission wavelengths were fixed at 275 and 305 nm, respectively, slits were set to 5 nm. The signal accumulation time was 1 s, the optimal *g*-factor was preliminary determined as 2.0. Measurements were performed in the automatic antiphotobleaching mode. The dissociation mixture was under constant stirring at the maximum rate provided by the FluoroMax-4. The measurement cell was kept at +37 °C controlled by the temperature bath (Colora, Ultrathermostat, NB/DS-638).

■ ASSOCIATED CONTENT

Supporting Information

The Supporting Information is available free of charge on the ACS Publications website at DOI: 10.1021/jacs.5b08694.

Experimental procedures for the peptide purification, sample preparation for dissociation assays and solid-state NMR spectroscopy measurements, TEM imaging procedure, and details about the analytical RP-HPLC (PDF)

■ AUTHOR INFORMATION

Corresponding Author

*roland.riek@phys.chem.ethz.ch

Present Addresses

[§]Department of Chemical Engineering and Biotechnology, University of Cambridge, New Museums Site, Pembroke Street, Cambridge, CB2 3RA, U.K., nn282@cam.ac.uk.

[∥]Department of Biochemistry, University of Cambridge, Hopkins Building, Downing Site, Tennis Court Road, Cambridge, CB2 1QW, U.K., kb601@cam.ac.uk.

Notes

The authors declare no competing financial interest.

[⊥]Mannitol, which is the linear fully hydrogenated polyol, is considered together with other LMW cyclic carbohydrates for simplicity.

■ ACKNOWLEDGMENTS

The authors would like to thank the members of the Riek group, especially Dr. J. Greenwald, Dr. S. Campioni, and Dr. C. Eichmann, for valuable discussions and support with daily maintenance of the laboratory equipment. $A\beta_{1-42}$ fibrils were kindly provided by Dr. M. Wälti. Special acknowledgement is addressed to P. Tittmann (EMEZ, ETH Zurich) for his help in TEM measurements. The access to MS instruments was kindly provided by Prof. Dr. R. Zenobi from LOC ETH Zurich. The authors are thankful to Prof. Dr. M. Morbidelli from ICBI ETH Zurich for giving an access to Enspire Multilabel Plate Reader. We are greatly thankful to Dr. J. Gallop (the Gurdon Institute, Cambridge University, U.K.) for generous access to Fluoromax-4 spectrofluorometer. We would like to thank Ashley Fidler for editing parts of the manuscript and providing excellent advice on how to write clear in English. This work was supported by ETH Zurich and the Swiss National Science Foundation (Grants 200020_126488, 200020_146757, and 200020_159707).

■ REFERENCES

(1) Chiti, F.; Dobson, C. M. In *Annu. Rev. Biochem.* **2006**; Vol. *75*, p 333.10.1146/annurev.biochem.75.101304.123901

(2) Blanco, L. P.; Evans, M. L.; Smith, D. R.; Badtke, M. P.; Chapman, M. R. *Trends Microbiol.* **2012**, *20*, 66.

(3) King, C. Y.; Tittmann, P.; Gross, H.; Gebert, R.; Aebi, M.; Wuthrich, K. *Proc. Natl. Acad. Sci. U. S. A.* **1997**, *94*, 6618.

(4) Coustou, V.; Deleu, C.; Saupe, S.; Begueret, J. *Proc. Natl. Acad. Sci. U. S. A.* **1997**, *94*, 9773.

(5) Seuring, C.; Greenwald, J.; Wasmer, C.; Wepf, R.; Saupe, S. J.; Meier, B. H.; Riek, R. *PLoS Biol.* 2012, *10*.

(6) Fowler, D. M.; Koulov, A. V.; Alory-Jost, C.; Marks, M. S.; Balch, W. E.; Kelly, J. W. *PLoS Biol.* **2005**, *4*, 100.

(7) Berson, J. F.; Harper, D. C.; Tenza, D.; Raposo, G.; Marks, M. S. *Mol. Biol. Cell* **2001**, *12*, 3451.

(8) Maji, S. K.; Perrin, M. H.; Sawaya, M. R.; Jessberger, S.; Vadodaria, K.; Rissman, R. A.; Singru, P. S.; Nilsson, K. P. R.; Simon, R.; Schubert, D.; Eisenberg, D.; Rivier, J.; Sawchenko, P.; Vale, W.; Riek, R. *Science* **2009**, *325*, 328.

(9) Faller, A.; Schünke, M.; Schünke, G.; Taub, E. *The Human Body: An Introduction to Structure and Function*; Thieme: Stuttgart, Germany, 2004.

(10) Lehninger, A. L.; Nelson, D. L.; Cox, M., 4th ed.; Palgrave Macmillan Limited: London, 2004.

(11) Alberts, B.; Johnson, A.; Lewis, J.; Raff, M.; Roberts, K.; Walter, P. *Molecular Biology of the Cell*, 5th ed.; Garland Science: New York, NY, 2008.

(12) Glombik, M. M.; Gerdes, H.-H. *Biochimie* **2000**, *82*, 315.

(13) Borgonovo, B.; Ouwendijk, J.; Solimena, M. *Curr. Opin. Cell Biol.* **2006**, *18*, 365.

(14) Dannies, P. S. *Endocr. Rev.* **1999**, *20*, 3.

(15) Giannattasio, G.; Zanini, A.; Meldolesi, J. *J. Cell Biol.* **1975**, *64*, 246.

(16) Loh, Y. P.; Kim, T.; Rodriguez, Y. M.; Cawley, N. X. *J. Mol. Neurosci.* **2004**, *22*, 63.

(17) Schnabel, E.; Mains, R. E.; Farquhar, M. G. *Mol. Endocrinol.* **1989**, *3*, 1223.

(18) van den Pol, A. N. *Neuron* **2012**, *76*, 98.

(19) Oakley, A. E.; Perry, R. H.; Candy, J. M.; Perry, E. K. *Neuropeptides* **1981**, *2*, 1.

(20) Dannies, P. S. *Endocr. Rev.* **2012**, *33*, 254.

(21) Arvan, P.; Castle, D. *Biochem. J.* **1998**, *332*, 593.

(22) Hosaka, M.; Watanabe, T. *Endocr. J.* **2010**, *57*, 275.

(23) Hutton, J. C.; Penn, E. J.; Peshavaria, M. *Biochem. J.* **1983**, *210*, 297.

(24) Leblond, F. A.; Viau, G.; Laine, J.; Lebel, D. *Biochem. J.* **1993**, *291*, 289.

(25) Colomer, V.; Kicska, G. A.; Rindler, M. J. *J. Biol. Chem.* **1996**, *271*, 48.

(26) Jain, R. K.; Joyce, P. B. M.; Gorr, S. U. *J. Biol. Chem.* **2000**, *275*, 27032.

(27) Gerdes, H. H.; Rosa, P.; Phillips, E.; Baeuerle, P. A.; Frank, R.; Argos, P.; Huttner, W. B. *J. Biol. Chem.* **1989**, *264*, 12009.

(28) Vonzastrow, M.; Castle, J. D. *J. Cell Biol.* **1987**, *105*, 2675.

(29) Radosevich, P. M.; Nash, J. A.; Lacy, D. B.; Odonovan, C.; Williams, P. E.; Abumrad, N. N. *Brain Res.* **1989**, *498*, 89.

(30) Duncan, R. R.; Greaves, J.; Wiegand, U. K.; Matskevich, I.; Bodammer, G.; Apps, D. K.; Shipston, M. J.; Chow, R. H. *Nature* **2003**, *422*, 176.

DOI: 10.1021/jacs.5b08694
J. Am. Chem. Soc. 2016, 138, 846−856

(31) Schmidt, R. F.; Lang, F.; Heckmann, M. *Physiologie Des Menschen: Mit Pathophysiologie*; Springer: London, Ltd., 2005.
(32) Koolman, J.; Röhm, K.-H.; Wirth, J. *Color Atlas of Biochemistry*, 2nd ed. rev. and enlarged ed.; Thieme, Stuttgart, 2005.
(33) Paroutis, P.; Touret, N.; Grinstein, S. *News Physiol. Sci.* **2004**, *19*, 207.
(34) McGlinchey, R. P.; Gruschus, J. M.; Nagy, A.; Lee, J. C. *Biochemistry* **2011**, *50*, 10567.
(35) Greenwald, J.; Riek, R. *Structure* **2010**, *18*, 1244.
(36) Kolset, S. O.; Prydz, K.; Pejler, G. *Biochem. J.* **2004**, *379*, 217.
(37) Lagunoff, D.; Rickard, A. *Am. J. Pathol.* **1999**, *154*, 1591.
(38) Jackson, R. L.; Busch, S. J.; Cardin, A. D. *Physiol. Rev.* **1991**, *71*, 481.
(39) Luppi, E.; Cesaretti, M.; Volpi, N. *Biomacromolecules* **2005**, *6*, 1672.
(40) Engelberg, H. *Circulation* **1961**, *23*, 578.
(41) Dalayeun, J. F.; Nores, J. M.; Bergal, S. *Biomed. Pharmacother.* **1993**, *47*, 311.
(42) Bodnar, R. J. *Peptides* **2014**, *62*, 67.
(43) Ablimit, A.; Kühnel, H.; Strasser, A.; Upur, H. *Chin. J. Integr. Med.* **2013**, *19*, 603.
(44) Font, L.; Luján, M. Á.; Pastor, R. *Front. Behav. Neurosci.* **2013**, *7*, 93.
(45) Börner, C.; Lanciotti, S.; Koch, T.; Höllt, V.; Kraus, J. *J. Neuroimmunol.* **2013**, *263*, 35.
(46) Misra, U. K.; Kalita, J.; Tripathi, G. M.; Bhoi, S. K. *Cephalalgia* **2013**, *33*, 316.
(47) Pritchard, L. E.; White, A. *Endocrinology* **2007**, *148*, 4201.
(48) Lee, C.-C.; Nayak, A.; Sethuraman, A.; Belfort, G.; McRae, G. J. *Biophys. J.* **2007**, *92*, 3448.
(49) Zhang, S.; Andreasen, M.; Nielsen, J. T.; Liu, L.; Nielsen, E. H.; Song, J.; Ji, G.; Sun, F.; Skrydstrup, T.; Besenbacher, F.; Nielsen, N. C.; Otzen, D. E.; Dong, M. *Proc. Natl. Acad. Sci. U. S. A.* **2013**, *110*, 2798.
(50) Wilcken, R.; Wang, G.; Boeckler, F. M.; Fersht, A. R. *Proc. Natl. Acad. Sci. U. S. A.* **2012**, *109*, 13584.
(51) Nielsen, S. B.; Franzmann, M.; Basaiawmoit, R. V.; Wimmer, R.; Mikkelsen, J. D.; Otzen, D. E. *Biopolymers* **2010**, *93*, 678.
(52) Nielsen, S. B.; Yde, P.; Giehm, L.; Sundbye, S.; Christiansen, G.; Mathiesen, J.; Jensen, M. H.; Jensen, P. H.; Otzen, D. E. *J. Mol. Biol.* **2012**, *421*, 601.
(53) Campioni, S.; Carret, G.; Jordens, S.; Nicoud, L.; Mezzenga, R.; Riek, R. *J. Am. Chem. Soc.* **2014**, *136*, 2866.
(54) Nielsen, L.; Khurana, R.; Coats, A.; Frokjaer, S.; Brange, J.; Vyas, S.; Uversky, V. N.; Fink, A. L. *Biochemistry* **2001**, *40*, 6036.
(55) D'Amico, M.; Di Carlo, M. G.; Groenning, M.; Militello, V.; Vetri, V.; Leone, M. *J. Phys. Chem. Lett.* **2012**, *3*, 1596.
(56) Cloe, A. L.; Orgel, J. P. R. O.; Sachleben, J. R.; Tycko, R.; Meredith, S. C. *Biochemistry* **2011**, *50*, 2026.
(57) Wang, L.; Maji, S. K.; Sawaya, M. R.; Eisenberg, D.; Riek, R. *PLoS Biol.* **2008**, *6*, 1791.
(58) Groenning, M. *J. Chem. Biol.* **2010**, *3*, 1.
(59) Sabaté, R.; Lascu, I.; Saupe, S. J. *J. Struct. Biol.* **2008**, *162*, 387.
(60) Munishkina, L. A.; Henriques, J.; Uversky, V. N.; Fink, A. L. *Biochemistry* **2004**, *43*, 3289.
(61) Campioni, S.; Mannini, B.; López-Alonso, J. P.; Shalova, I. N.; Penco, A.; Mulvihill, E.; Laurents, D. V.; Relini, A.; Chiti, F. *J. Mol. Biol.* **2012**, *424*, 132.
(62) Marek, P. J.; Patsalo, V.; Green, D. F.; Raleigh, D. P. *Biochemistry* **2012**, *51*, 8478.
(63) Pedersen, J. S.; Flink, J. M.; Dikov, D.; Otzen, D. E. *Biophys. J.* **2006**, *90*, 4181.
(64) Hayat, M. A. *General Methods and Overviews, Lung Carcinoma and Prostate Carcinoma*; Springer, Dordrecht, 2008; Vol. 2.
(65) Takegoshi, K.; Nakamura, S.; Terao, T. *Chem. Phys. Lett.* **2001**, *344*, 631.
(66) Kunz, W. *Curr. Opin. Colloid Interface Sci.* **2010**, *15*, 34.
(67) Kunz, W. *Specific Ion Effects*; World Scientific, Singapore, 2010.
(68) McIlvaine, T. C. *Mon. Weather Rev.* **1921**, *49*, 183.
(69) Foster, M. C.; Leapman, R. D.; Li, M. X.; Atwater, I. *Biophys. J.* **1993**, *64*, 525.
(70) ProteinCalculator v3.4. http://protcalc.sourceforge.net/.
(71) Fung, J.; Darabie, A. A.; McLaurin, J. *Biochem. Biophys. Res. Commun.* **2005**, *328*, 1067.
(72) Macchi, F.; Eisenkolb, M.; Kiefer, H.; Otzen, D. E. *Int. J. Mol. Sci.* **2012**, *13*, 3801.
(73) Noborn, F.; O'Callaghan, P.; Hermansson, E.; Zhang, X.; Ancsin, J. B.; Damas, A. M.; Dacklin, I.; Presto, J.; Johansson, J.; Saraiva, M. J.; Lundgren, E.; Kisilevsky, R.; Westermark, P.; Li, J.-P. *Proc. Natl. Acad. Sci. U. S. A.* **2011**, *108*, 5584.
(74) Cohlberg, J. A.; Li, J.; Uversky, V. N.; Fink, A. L. *Biochemistry* **2002**, *41*, 1502.
(75) Madine, J.; Davies, H. A.; Hughes, E.; Middleton, D. A. *Biochemistry* **2013**, *52*, 8984.
(76) Yamaguchi, I.; Suda, H.; Tsuzuike, N.; Seto, K.; Seki, M.; Yamaguchi, Y.; Hasegawa, K.; Takahashi, N.; Yamamoto, S.; Gejyo, F.; Naiki, H. *Kidney Int.* **2003**, *64*, 1080.
(77) Seuring, C. *ETH*; ETH: Zürich, 2012.
(78) Lindman, S.; Linse, S.; Mulder, F. A. A.; Andre, I. *Biochemistry* **2006**, *45*, 13993.
(79) Hatters, D. M.; Minton, A. P.; Howlett, G. J. *J. Biol. Chem.* **2002**, *277*, 7824.
(80) Minton, A. P. *Biophys. J.* **2001**, *80*, 1641.
(81) In *Principles of Fluorescence Spectroscopy*; Lakowicz, J., Ed.; Springer: New York, 2006; p 353.
(82) In *Biophys. Chem.*, 1st ed.; Cantor, C. R., Schimmel, P. R., Eds.; W.H. Freeman: San Francisco, 1980; Vol. 2, p 365.
(83) Schwarz, L.; Kindermann, W. *Eur. J. Appl. Physiol. Occup. Physiol.* **1990**, *61*, 165.
(84) Xue, Y.; Lee, S.; Ha, Y. *Proc. Natl. Acad. Sci. U. S. A.* **2011**, *108*, 16229.

DOI: 10.1021/jacs.5b08694
J. Am. Chem. Soc. 2016, 138, 846−856